

# Universal dynamics far from equilibrium in Heisenberg ferromagnets

Saraswat Bhattacharyya, Joaquin F. Rodriguez-Nieva, and Eugene Demler  
*Department of Physics, Harvard University, Cambridge, MA 02138, USA*

We study the universal far from equilibrium dynamics of magnons in Heisenberg ferromagnets. We show that such systems exhibit universal scaling in momentum and time of the quasiparticle distribution function, with the universal exponents distinct from those recently observed in Bose-Einstein condensates. This new universality class originates from the  $SU(2)$  symmetry, which results in a strong momentum-dependent magnon-magnon scattering amplitude and absence of collisions between magnons and the condensate. We compute the universal exponents using the Boltzmann kinetic equation and incoherent initial conditions that can be realized with microwave pumping of magnons. We compare our numerical results with the analytic scaling solution, and demonstrate the robustness of the scaling to variations in the initial conditions. Our predictions can be tested in quench experiments of spin systems in optical lattices and pump-probe experiments in thin-layered ferromagnets such as Yttrium Iron Garnet.

**Introduction.** Understanding how universal behavior emerges in interacting quantum systems far from equilibrium is a central question in theoretical physics. A large body of theoretical works have proposed that isolated quantum systems, such as quark-gluon plasma after heavy ion collision, the early universe after inflation, or cold atoms after a quench, can exhibit universal behavior as they evolve far from equilibrium[1–13]. Such behavior is manifested in universal scaling in time and momenta of correlation functions in the prethermal regime, with the universal exponents independent of microscopic details or initial conditions. The appearance of universality far from equilibrium can be attributed to the existence of non-thermal fixed points in the system’s phase space (Fig.1), with the non-equilibrium state inheriting its universal exponents[14]. Manifestations of universality far from equilibrium were recently observed experimentally for the first time in cold atomic gases[15–17]. This experimental feat creates new challenges, both in classifying all the possible universality classes as well as devising new tabletop experiments to explore them.

Here we uncover a new universality class arising in Heisenberg ferromagnets in the presence of  $SU(2)$  symmetry. Similar to the case observed experimentally with an interacting Bose-Einstein condensate (BEC) [15–17], the prethermal quasiparticle distribution acquires a self-similar form:

$$n_{\mathbf{k}}(t) = t^\alpha f(t^\beta |\mathbf{k}|), \quad (1)$$

where  $\alpha$  and  $\beta$  are universal exponents independent of microscopic details or initial conditions, and  $f(x)$  is a universal function. Key properties that determine  $\alpha$  and  $\beta$  are dimensionality, quasiparticle dispersion, and the nature of interactions. While a ferromagnet at low energy is effectively an interacting Bose gas after a Holstein-Primakoff transformation[18], the presence of  $SU(2)$  symmetry sets them apart from a conventional BEC in two important ways. First, interaction between quasiparticles are strongly constrained by  $SU(2)$  symmetry, giving

rise to ‘soft’ collisions [Eq.(4) below]. Second, the  $SU(2)$  symmetry hinders collisions between quasiparticles and the condensate. These two features lead to distinct universal exponents in a broad range of wavevectors.

Crucially, we find that the key requirement for the observation of the universal scaling in Eq.(1) is that a sufficiently large population of magnons is pumped into the system in order to drive a swift transition into the self-similar prethermal regime — the details of the initial conditions are unimportant. For example, assuming that magnons (which have quadratic dispersion in ferromagnets) are pumped in an energy window centered at  $\omega$  and width  $\Delta\omega \sim \omega$ , then the density of magnons  $\rho$  has to satisfy  $\rho a^d \gg (\omega/J)^{d/2}$ , with  $a$  the lattice constant,  $J$  the exchange coupling and  $d$  is the system’s dimension, such that the occupation number of modes at frequency  $\omega$  is  $n_\omega \gg 1$ , see Fig.1 (note that  $\rho a^d$  has an upper bound  $2S + 1$  for a spin- $S$  system). Below such magnon density threshold, we do not observe self-similarity and the system evolves directly into the thermal fixed point.

Thermalization dynamics in Heisenberg ferromagnets also features other interesting characteristics besides self-

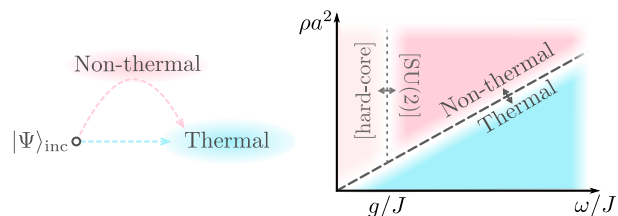


FIG. 1. The presence of non-thermal fixed points in phase space can induce a prethermal state. Whether such state is formed starting from an incoherent state  $|\Psi\rangle_{\text{inc}}$  depends on the total density  $\rho$  of magnons pumped into the system, and the frequency  $\omega$  at which they are pumped. Both  $\rho$  and  $\omega$  can be controlled through the strength and frequency of the driving field (see Fig.2). Here  $J$  is the exchange coupling,  $g$  is the interaction strength which break the  $SU(2)$  symmetry, and  $a$  is the lattice constant.

similar behavior. In particular, the SU(2) symmetry hinders thermalization of magnons at small momenta, thus creating a bottleneck for magnon relaxation. This is supported by previous experimental studies in the context of Bose-Einstein condensation of magnons in Yttrium Iron Garnet (YIG) after microwave pumping[19–21]. These experiments found a thermalization time  $\tau \sim 10 - 100$  ns, which is surprisingly slow given that the exchange coupling  $J$  is on the THz scale. Similarly to how thermalization in close to integrable systems is governed by integrability-breaking terms[22–24], we show that thermalization of long wavelength modes in ferromagnets is governed by terms that break the SU(2) symmetry, such as dipolar interactions or easy axis/plane anisotropies.

Besides of its fundamental appeal, our predictions are relevant in a variety of ongoing experiments. For example, we argue that the universal scaling exponents can be accessed in the previously-mentioned experiments in YIG [19–21, 25, 26] despite the coupling with phonons or SU(2) symmetry breaking processes. As shown below, collisions between quasiparticles due to exchange coupling,  $J \sim 100$  meV, can be made much faster than processes which lead to energy or quasiparticle losses, such as dipolar interactions  $g \lesssim 1$  meV, if magnons with sufficiently large energies are populated ( $\omega \gg g$ ). Cold atom platforms are also promising because the system can be effectively isolated from the environment, and the exchange interaction can be engineered using various mechanisms, *e.g.* Feshbach resonances, dipolar interactions or lattice shaking to name a few[27–33].

**Microscopic model.** We consider a two-dimensional Heisenberg ferromagnet on a square lattice with nearest-neighbor exchange coupling  $J$  and Zeeman field  $h_z$ :

$$\hat{\mathcal{H}} = -J \sum_{\langle jj' \rangle} \hat{S}_j \cdot \hat{S}_{j'} + h_z \sum_j \hat{S}_j^z. \quad (2)$$

Here  $\sum_{\langle jj' \rangle}$  denotes summation over nearest neighbors. We assume that the system has  $N$  lattice sites, each containing a spin  $S$  degree of freedom, and periodic boundary conditions in each spatial direction. The spin operators satisfy the commutation relations  $[\hat{S}_j^z, \hat{S}_{j'}^\pm] = \pm \delta_{jj'} \hat{S}_j^\pm$ , and  $[\hat{S}_j^+, \hat{S}_{j'}^-] = 2\delta_{jj'} \hat{S}_j^z$ , with  $\hat{S}_j^\pm = \hat{S}_j^x \pm i\hat{S}_j^y$ .

We proceed to build an effective theory valid when the density of quasiparticles is small,  $\rho a^2 \ll 1$ . We recall that one magnon states  $|\mathbf{k}\rangle = \hat{S}_{\mathbf{k}}^+ |F\rangle$  are exact eigenstates of  $\hat{\mathcal{H}}$  with energies

$$\varepsilon_{\mathbf{k}} = h_z + JS(\gamma_0 - \gamma_{\mathbf{k}}), \quad \gamma_{\mathbf{k}} = \sum_{\tau} e^{i\mathbf{k}\cdot\boldsymbol{\tau}}. \quad (3)$$

Here  $|F\rangle = |\downarrow\downarrow \dots \downarrow\rangle$  denotes the ferromagnetic ground state and  $\hat{S}_{\mathbf{k}}^+$  denotes  $\hat{S}_{\mathbf{k}}^+ = \frac{1}{\sqrt{N}} \sum_j e^{-i\mathbf{k}\cdot\boldsymbol{\tau}_j} \hat{S}_j^+$ . Two magnon states  $|\mathbf{k}, \mathbf{p}\rangle = \frac{1}{2S} \hat{S}_{\mathbf{k}}^+ \hat{S}_{\mathbf{p}}^+ |F\rangle$ , however, are *not* eigenstates of  $\hat{\mathcal{H}}$ . [18, 34] The interaction between

magnons can be obtained from the matrix elements

$$\begin{aligned} \hat{\mathcal{H}}|\mathbf{k}, \mathbf{p}\rangle &= (\varepsilon_{\mathbf{k}} + \varepsilon_{\mathbf{p}})|\mathbf{k}, \mathbf{p}\rangle + \sum_{\mathbf{q}} G_{\mathbf{k}, \mathbf{p}}^{\mathbf{q}} |\mathbf{k} + \mathbf{q}, \mathbf{p} - \mathbf{q}\rangle, \\ G_{\mathbf{k}, \mathbf{p}}^{\mathbf{q}} &= \frac{J}{N} (\gamma_{\mathbf{q}-\mathbf{p}} + \gamma_{\mathbf{q}+\mathbf{k}} - \gamma_{\mathbf{q}} - \gamma_{\mathbf{k}+\mathbf{q}-\mathbf{p}}), \end{aligned} \quad (4)$$

such that one magnon states are coupled via momentum-conserving collision  $G_{\mathbf{k}, \mathbf{p}}^{\mathbf{q}}$ . When the incoming magnons have long wavelength, the collision term takes the simple form  $G_{\mathbf{k}, \mathbf{p}}^{\mathbf{q}} \approx -\frac{Ja^2}{N} (\mathbf{k} \cdot \mathbf{p})$ . This characteristic  $(\mathbf{k} \cdot \mathbf{p})$  interaction arises from the global SU(2) symmetry and justifies why magnons propagate ballistically when  $|\mathbf{k}| \rightarrow 0$ . Such soft collision may seem counterintuitive for  $S = 1/2$  systems given that two local spin flips are forbidden, which then suggests a strong hard-core interaction in order to prevent having two excitations on the same lattice site. Hard core collisions (and magnon leakage), however, may arise if the SU(2) symmetry is broken. Here we will focus on the regime in which the characteristic magnon wavevector  $k_*$  (which is controlled by the frequency of pumping) satisfies  $J(k_*a)^2 \gg g$ , with  $g$  the strength of the SU(2) symmetry breaking term, such that the system is effectively SU(2) symmetric.

For a small magnon density such that the probability of having three or more magnons in close proximity is small, the magnon gas can be described as a bose gas with kinetic energy  $\varepsilon_{\mathbf{k}}$ , Eq.(3), and the two-body interaction  $G_{\mathbf{k}, \mathbf{p}}^{\mathbf{q}}$  in Eq.(4). For  $\omega \ll J$ , only small  $\mathbf{k}$  vectors are occupied, and we can expand the kinetic and interaction terms at small momenta as:

$$\hat{\mathcal{H}} = \sum_{\mathbf{k}} \varepsilon_{\mathbf{k}} \hat{a}_{\mathbf{k}}^\dagger \hat{a}_{\mathbf{k}} - \frac{Ja^2}{N} \sum_{\mathbf{k}, \mathbf{p}, \mathbf{q}} (\mathbf{k} \cdot \mathbf{p}) \hat{a}_{\mathbf{p}+\mathbf{q}}^\dagger \hat{a}_{\mathbf{k}-\mathbf{q}}^\dagger \hat{a}_{\mathbf{p}} \hat{a}_{\mathbf{k}} + h.c. \quad (5)$$

In our discussion, we assume that the lattice is at a small temperature such that magnon-phonon interactions can be neglected, which is usually the case for the timescales of interest  $t \lesssim 1 \mu\text{s}$  [35, 36].

In contrast to the Bogoliubov theory of weakly interacting Bose particles, the Hamiltonian (5) does not have anomalous terms of the form  $a_{-\mathbf{k}}^\dagger a_{\mathbf{k}}^\dagger$  which describe coherent scattering between finite energy quasiparticles and the condensate. Furthermore, scattering of quasiparticles vanishes as their momentum approaches zero, which precludes the formation of a magnon condensate at  $\mathbf{k} = 0$ . These properties justify why a kinetic description at intermediate/long times is valid: the lack of condensate formation at low momenta would otherwise give rise to non-perturbative corrections at sufficiently long times.

**Initial conditions** We supplement the model in Eq. (5) with initial conditions which are relevant in a variety of non-equilibrium studies of ferromagnets, namely, uniform incoherent pumping of magnons in a narrow band of energies centered around  $\omega$  satisfying  $\omega > h_z$ . As shown in Fig.2, one way to achieve such initial conditions in a ferromagnetic material such as YIGs is via transverse

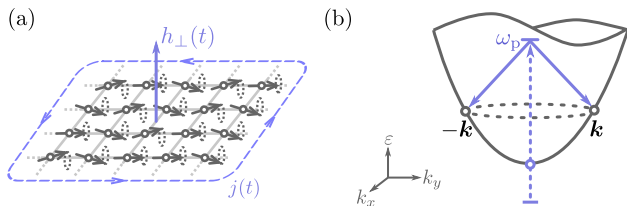


FIG. 2. (a) Schematics of transverse pumping of magnons in a two-dimensional ferromagnet using a uniform time-dependent magnetic field  $h_{\perp}(t)$ , e.g. through an AC current  $j(t)$ . (b) Shown is the creation of coherent pairs  $(\mathbf{k}, -\mathbf{k})$ , with  $\varepsilon_{\mathbf{k}} = \omega_p/2$ , using microwave pumping at frequency  $\omega_p$ . Here we assume the presence of a weak dipole-dipole interaction in the system. The number (energy) of magnons pumped into the modes  $\mathbf{k}$  can be controlled with the strength (frequency) of  $h_{\perp}(t)$ .

microwave pumping  $h_{\perp}(t)$  at frequency  $\omega_p = 2\varepsilon_{\mathbf{k}}$ [37]. This protocol assumes that there is a finite dipole-dipole interaction [but small compared to  $J(k_*, a)^2$ ]. The amount of magnons pumped into the systems can be controlled by the strength of  $h_{\perp}$ , giving two independent knobs to control which  $\mathbf{k}$  modes are excited, and their respective population  $n_{\mathbf{k}}$ . Although parametric pumping of magnons also create anomalous correlations  $\langle \hat{a}_{-\mathbf{k}}^{\dagger} \hat{a}_{\mathbf{k}}^{\dagger} \rangle$ , these decohere rapidly since pairs with different wavevectors  $\mathbf{k}$  oscillate with different frequencies. We also note that this protocol leads to no net spin texture,  $\langle \hat{S}_{\mathbf{k}}^{x,y} \rangle = 0$ .

With this picture in mind, we parametrize the initial condition for Eq.(7) as

$$n_{\mathbf{k}}(t=0) = \frac{n_* \Gamma^2}{(|\mathbf{k}| - k_*)^2 + \Gamma^2}, \quad (6)$$

where  $k_*$  is the wavevector at which magnons are pumped ( $\omega = k_*^2/2m$ ),  $n_*$  parametrizes the number of magnons pumped into the system, and  $\Gamma$  determines the initial width of the distribution (its value depends on the details of the pump pulse, e.g. its duration). We emphasize that, although  $n_{\mathbf{k}}$  can be much larger than 1,  $n_*$  needs to be chosen such that  $\rho a^2 \ll 1$  for Eq.(5) to be valid.

**Equations of motion.** The measurable quantity of interest is the magnon population  $n_{\mathbf{k}}(t) = \langle \hat{S}_{-\mathbf{k}}^+(t) \hat{S}_{\mathbf{k}}^-(t) \rangle$  as a function of time. In ferromagnetic materials, such quantity can be measured via Brillouin scattering, which was previously used in the context of Bose-Einstein condensation in YIG[20, 21]. An alternative technique is spin qubit magnetometry[38], which has been used to measure (steady-state) magnon population[39, 40] as well as imaging single spins[41], but also has been proposed to access a variety of elementary excitations in ferromagnets[42, 43], spin ice[44], spin chains[45], and spin liquids[46]. In cold atom experiments, it is possible to use snapshots of local spin measurements  $\langle \hat{S}_i^x \hat{S}_j^x \rangle$  for the different spin pairs in order to compute  $n_{\mathbf{k}}$ .

The time evolution of  $n_{\mathbf{k}}(t)$  at intermediate/long time

scales can be described using the kinetic equation in the weak scattering regime, which is justified by the soft collisions in Eq.(5):

$$\partial_t n_{\mathbf{k}} = I_{\mathbf{k}} \{n_{\mathbf{p}}\}. \quad (7)$$

Here  $I_{\mathbf{k}}$  the collision integral

$$I_{\mathbf{k}} = J^2 a^4 \sum_{\mathbf{p}\mathbf{q}} (\mathbf{k} \cdot \mathbf{p})^2 \left[ n_{\mathbf{k}} n_{\mathbf{p}} (1 + n_{\mathbf{k}+\mathbf{q}}) (1 + n_{\mathbf{p}-\mathbf{q}}) - (1 + n_{\mathbf{k}}) (1 + n_{\mathbf{p}}) n_{\mathbf{k}+\mathbf{q}} n_{\mathbf{p}-\mathbf{q}} \right] \delta(\varepsilon_i - \varepsilon_f), \quad (8)$$

with  $\varepsilon_i = \varepsilon_{\mathbf{k}} + \varepsilon_{\mathbf{p}}$  and  $\varepsilon_f = \varepsilon_{\mathbf{k}+\mathbf{q}} + \varepsilon_{\mathbf{p}-\mathbf{q}}$  the energies of the initial and final states, respectively. In using the kinetic equation (7) and (8), we are implicitly assuming that decoherence of anomalous terms has already occurred. Starting from the initial conditions in Eq.(6), we numerically solve Eqs.(7)-(8).

#### Universal exponents from dimensional analysis.

Before presenting numerical results of the kinetic equation, we discuss the analytical results for the expected scaling exponent[47, 48]. Using the self-similar ansatz in Eq.(1) and defining  $\kappa_i \equiv t^{\beta} k_i$ , the left-hand-side of Eq.(7) reads  $\partial_t n_{\mathbf{k}} = t^{\alpha-1} [\alpha f(|\kappa|) + \beta \kappa f'(|\kappa|)]$ . In the region of momentum space in which  $n_{\mathbf{k}} \gg 1$  [i.e., cubic terms of  $n_{\mathbf{k}}$  in Eq.(7) dominate], the right-hand-side of Eq.(7) reads  $I_{\mathbf{k}} \{n_{\mathbf{p}}\} = t^{3\alpha-4\beta-2d\beta+2\beta} I_{\kappa} \{f(|\kappa|)\}$ . Matching the coefficients of  $t$  on both sides of Eq.(7), we find

$$2(d+1)\beta - 2\alpha = 1. \quad (9)$$

The second relation between  $\alpha$  and  $\beta$  can be found from conservation laws. Because magnon number is conserved after the pump, the condition  $\rho = \int \frac{d^d \mathbf{k}}{(2\pi)^d} n_{\mathbf{k}}(t) = t^{\alpha-\beta d} \int d^d \kappa f(\kappa)$  leads to:

$$\alpha = \beta d. \quad (10)$$

For  $d=2$ , Eqs.(9)-(10) suggest that  $\alpha = 1$  and  $\beta = 0.5$ , which are close to the values found numerically below. We stress that such scaling is expected to be valid at intermediate momenta  $|\mathbf{k}| \approx k_*$  where  $n_{\mathbf{k}} \gg 1$ . At large momenta,  $|\mathbf{k}| \gg k_*$ , the self-similar scaling is no longer valid because  $n_{\mathbf{k}} \lesssim 1$ . At small momenta,  $|\mathbf{k}| \ll k_*$ , the evolution is governed by a negligible scattering rate.

As a side remark, we note that we could have assumed energy conservation, which leads to the condition  $\alpha = (\beta+2)d$ , rather than particle number conservation which lead to Eq. (10). Whether particle number or energy conservation dominates in the self-similar region has to be checked empirically by numerical simulations.

#### Universal exponents from kinetic simulations.

We first focus on prethermalization in the large pumping regime,  $n_* \gg 1$ . As shown in Fig.3(a), after a few timesteps in units of  $\tau_*$ ,

$$\tau_* = \frac{J^2}{\omega^3 n_*^3}, \quad (11)$$

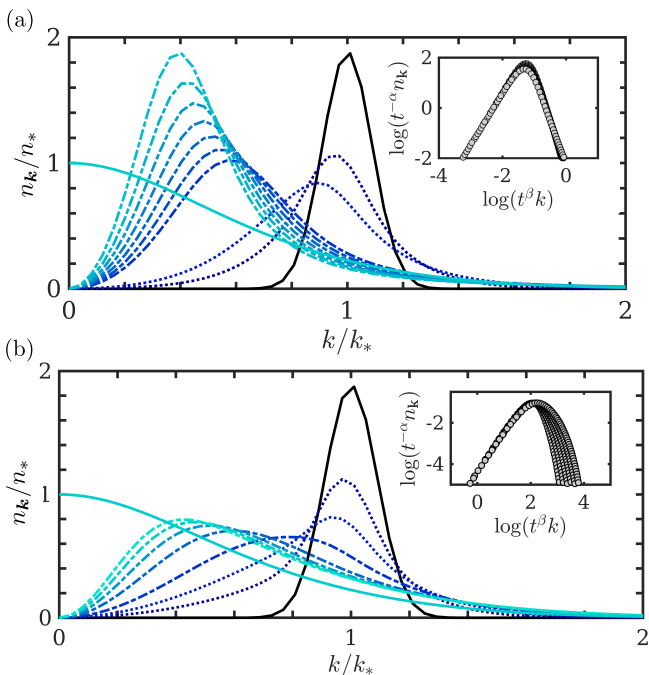


FIG. 3. Evolution of the occupation number  $n_{\mathbf{k}}$  starting from an initial incoherent pump at wavevector  $|\mathbf{k}| = k_*$ , with occupation (a)  $n_* \gg 1$  and (b)  $n_* = 1$  [see Eq.(6)]. Indicated with dashed-dotted lines is the distribution function once the details of the initial conditions are lost. The inset (a) illustrates the collapse of the data points using a self-similar distribution function of the form  $n_{\mathbf{k}}(t) \propto t^\alpha f(t^\beta |\mathbf{k}|)$ , with  $\alpha$  and  $\beta$  defined in Eq.(12). The inset (b) exhibits no collapse of the data points. Solid lines indicate the initial (black) and final Bose-Einstein (light blue) distribution of the magnon fluid. The distributions are plotted at times  $t/\tau_* = 0, 0.01, 0.02, 0.09, 0.11, 0.13, 0.16, 0.18, 0.22, 0.28, \infty$  for (a) and  $t/\tau'_* = 0, 0.01, 0.02, 0.5, 0.1, 0.15, 0.2, 0.25, \infty$  for (b), with decreasing tones of blue [ $\tau_*$  is defined in Eq.(11) and  $\tau'_* = J^2/\omega^3 n_*^2$ ]. Parameters used:  $n_* = 100$ ,  $\Gamma = 0.2k_*$  ( $\rho a^2 \approx 0.1$  if  $\omega/J = 0.01$ ).

the details of the initial conditions are lost and the distribution function at intermediate momenta,  $|\mathbf{k}| \sim k_*$ , acquires a self-similar form governed by Eq.(1). We find that the distribution function  $n_{\mathbf{k}}$  can be fitted by Eq.(1) in a broad range of momenta (between one and two decades) using the parameters

$$\alpha = 0.70 \pm 0.01, \quad \beta = 0.29 \pm 0.02, \quad (12)$$

and the universal function  $f(x) \sim 1/x^{2.3}$ . The uncertainty in Eq.(12) is obtained by initializing the simulation from qualitatively distinct initial conditions and computing the variations in  $(\alpha, \beta)$ , see below. Figure 3(a) also illustrates how the SU(2) symmetry affects thermalization at small momenta  $|\mathbf{k}| \ll k_*$ . This is manifested in the lack of scattering of magnon states at  $|\mathbf{k}| \approx 0$  due to the  $(\mathbf{k} \cdot \mathbf{p})$  scattering matrix element. For small momenta, the distribution function evolves as  $\partial_t n_{\mathbf{k}} \sim t|\mathbf{k}|^2$ . Such behavior is cutoff by terms that break SU(2) symmetry.

We emphasize that the exponents  $(\alpha, \beta)$  are distinct from those found experimentally in cold atom systems[15–17] (for instance,  $\alpha \approx \beta \approx 0.1$  in a 1D Bose-Einstein condensate in Ref.[15]). In addition to the difference in dimensionality, the key difference between the prethermal state observed in cold atoms and the one discussed in the present work is that, in the BEC case, dynamics is governed by collisions between quasiparticles and the condensate once the condensate starts to form.

In principle, nothing prevents observation of power law scaling of the distribution function when  $n_* \lesssim 1$ , i.e. weak pumping. As shown in Fig.3(b), we do not observe a self-similar scaling in our numerical results. In particular, we observe that the distribution at intermediate/large momenta relax to the thermal form  $n_{\mathbf{k}} \propto e^{-\varepsilon_{\mathbf{k}}/T}$  without exhibiting self-similarity (small momenta states,  $|\mathbf{k}| \ll k_*$ , still scales as  $n_{\mathbf{k}} \propto t|\mathbf{k}|^2$ ).

Importantly, the form of the prethermal solution is independent of the details of the initial condition. Figure 4(a) shows the evolution of the quasiparticle distribution after an initial pump at two frequencies. Similarly to Fig.3, the details of the initial conditions are lost in a time scale on the order of  $\tau_*$ , and the system evolves according to the self-similar solution in Eq.(1) with the universal exponents in Eq.(12).

**SU(2) symmetry breaking terms.** Interactions that break SU(2) symmetry allow to populate the long wavelength  $\mathbf{k} \approx 0$  modes. One such interaction that arise in typical systems are anisotropies in the exchange coupling,  $\hat{\mathcal{H}}_z = \delta J_z \sum_{\langle i,j \rangle} \hat{S}_i^z \hat{S}_j^z$ . It is straight-forward to show that  $\hat{\mathcal{H}}_z$  is effectively a hard-core interaction  $\hat{\mathcal{H}}_z = \frac{\delta J_z}{N} \sum_{\mathbf{k}, \mathbf{p}, \mathbf{q}} \hat{a}_{\mathbf{k}+\mathbf{q}}^\dagger \hat{a}_{\mathbf{p}-\mathbf{q}}^\dagger \hat{a}_{\mathbf{k}} \hat{a}_{\mathbf{p}}$ . If the anisotropy in the exchange coupling dominates, either because  $\delta J_z$  is large compared to  $J$  or because magnons are pumped close to the bottom of the band, then the critical exponents in Eq.(12) are no longer valid.

Another typical interaction is dipole-dipole interaction  $\hat{\mathcal{H}}_d = \frac{g_d a^3}{2} \sum_{jj'} \left[ \frac{\hat{\mathbf{S}}_j \cdot \hat{\mathbf{S}}_{j'}}{r_{jj'}^3} - \frac{3(\hat{\mathbf{S}}_j \cdot \mathbf{r}_{jj'})(\hat{\mathbf{S}}_{j'} \cdot \mathbf{r}_{jj'})}{r_{jj'}^5} \right]$  which is usually a small perturbation to Eq.(2) in solid-state materials, i.e.  $g_d \ll J$  ( $g_d = \mu_B^2/4\pi a^3$  is the dipolar energy, and  $\mu_B$  is the Bohr magneton). With  $\hat{\mathcal{H}}_d$  present, there are several possible behaviors depending on the canting angle  $\theta$  of the ferromagnetic order parameter with respect to the normal of the 2D plane which can be controlled via  $h_z$  in Eq.(2). For  $\theta = 0$ , dipolar interactions lead to the effective Hamiltonian  $\hat{\mathcal{H}}_d = -2g_d \sum_{\mathbf{k}} \hat{a}_{\mathbf{k}}^\dagger \hat{a}_{\mathbf{k}} + \frac{g_d}{N} \sum_{\mathbf{k}, \mathbf{p}, \mathbf{q}} \hat{a}_{\mathbf{k}+\mathbf{q}}^\dagger \hat{a}_{\mathbf{p}-\mathbf{q}}^\dagger \hat{a}_{\mathbf{k}} \hat{a}_{\mathbf{p}}$ . In this case, dipolar interactions is effectively hard core and the same conclusions as in the anisotropic exchange case follows. For  $0 < \theta \leq \pi/2$ , both cubic terms and anomalous terms arise, both of which do not preserve particle number. In this case, the collision integral (8) needs to be modified to account for the modified spectrum due to the Bogoliubov quasiparticles as well as three-particle

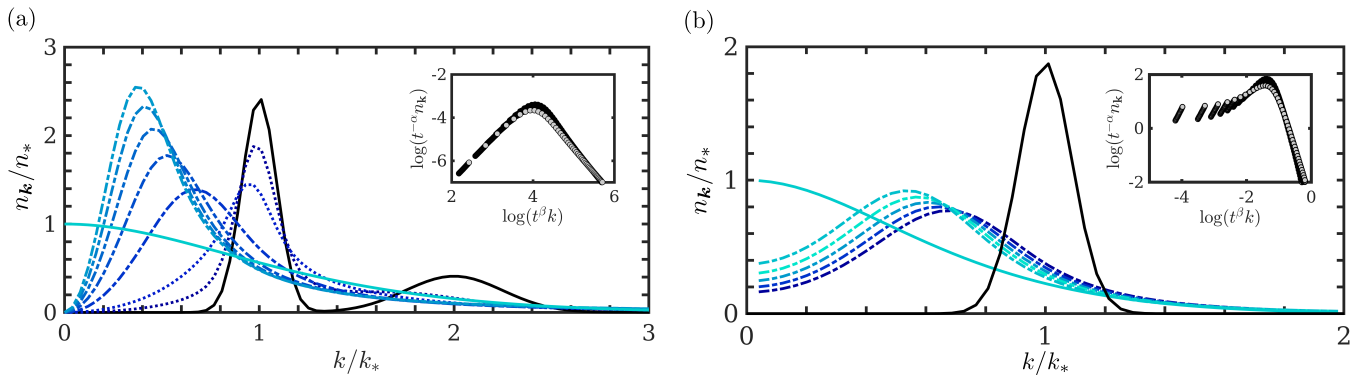


FIG. 4. (a) Robustness of the self-similar scaling under different initial conditions. Shown is the evolution of the quasiparticle distribution using a two-peak initial condition. In a time scale on the order  $\tau_*$ , the distribution function acquires a self-similar form such as the one observed in Fig.3. (b) Thermalization in the presence of SU(2) symmetry breaking terms which gives rise to scattering at small momenta. We do not observe a noticeable change in the  $(\alpha, \beta)$  values from those found in Eq.(12). Parameters used are described in the main text.

processes. Regardless of the presence of easy axis/plane anisotropies or dipolar interactions, these do not affect dynamics if magnons are pumped at sufficiently large energies,  $\omega \gg \max(g_d, J_z)$ .

To illustrate the effects of symmetry breaking interactions on thermalization, Fig.4(b) shows the magnon relaxation in the presence of hard-core collisions  $g = 0.05J(k_*a)^2$  and  $n_* \gg 1$ . Contrary to the previously studied cases, the  $\mathbf{k} \approx 0$  modes are populated at a speed on the order of  $\tau_g = \frac{J^2}{\omega g^2 n_*^3}$  which is larger than  $\tau_*$  in Eq.(11) by a factor of  $(\omega/g)^2$ . Importantly, we find that the universal exponents at intermediate momenta, where exchange interaction dominates, remain within the values found in Eq.(12).

**Summary & outlook.** We showed that Heisenberg ferromagnets exhibit universal behavior after an incoherent pump. One future direction to explore is whether other types of universal dynamics can emerge when we consider broader classes of initial conditions, for example, spin textures which are effectively a condensate at finite wavevector. In particular, spin textures induce effective interactions between quasiparticles and the condensate[49, 50]. Such question can be addressed using the formalism developed in Ref.[51]. Another direction is studying whether the self-similar scaling survives in the large magnon density regime, i.e. as we approach criticality. Such studies need to go beyond the kinetic equation, for instance, using Truncated Wigner Approximation for spin systems[52–54]. On the experimental front, probing the predicted non-thermal fixed point in ferromagnets is within grasp of ongoing experiments, namely driven ferromagnetic insulators and spins in optical lattices.

**Acknowledgements.** We thank C. Du, G. Falkovich, B. Halperin, J. Marino, A. Piñeiro Orioli, D. Podolsky, A. M. Rey, A. A. Rosch, D. Sels, A. Yacoby, T. Zhou

for enlightening discussions. We acknowledge support from Harvard-MIT CUA, NSF Grant No. DMR-1308435 and AFOSR-MURI: Photonic Quantum Matter (award FA95501610323).

- 
- [1] R. Micha and I. I. Tkachev, Phys. Rev. Lett. **90**, 121301 (2003).
  - [2] R. Micha and I. I. Tkachev, Phys. Rev. D **70**, 043538 (2004).
  - [3] J. Berges, S. Borsányi and C. Wetterich, Phys. Rev. Lett. **93**, 142002 (2004).
  - [4] J. Berges, D. Gelfand, and J. Pruschke, Phys. Rev. Lett. **107**, 061301 (2011).
  - [5] J. Berges, A. Rothkopf, and J. Schmidt, Phys. Rev. Lett. **101**, 041603 (2008).
  - [6] J. Berges and D. Sexty, Phys. Rev. D **83**, 085004 (2011).
  - [7] J. Berges, K. Boguslavski, S. Schlichting, R. Venugopalan, Phys. Rev. D **89**, 074011 (2014).
  - [8] A. Kurkela and G. D. Moore, Phys. Rev. D **86**, 056008 (2012).
  - [9] M. C. Abraao York, A. Kurkela, E. Lu, and G. D. Moore, Phys. Rev. D **89**, 074036 (2014).
  - [10] S. Schlichting, Phys. Rev. D **86**, 065008 (2012).
  - [11] J. Berges, K. Boguslavski, S. Schlichting, and R. Venugopalan, Phys. Rev. D **89**, 114007 (2014).
  - [12] A. Kurkela and E. Lu, Phys. Rev. Lett. **113**, 182301 (2014).
  - [13] A. Piñeiro Orioli, K. Boguslavski, and J. Berges, Phys. Rev. D **92**, 025041 (2015).
  - [14] J. Berges, arXiv:1503.02907.
  - [15] C. Eigen, *et al.*, Nature **563**, 221 (2018).
  - [16] S. Erne, R. Becker, T. Gasenzer, J. Berges, and J. Schmiedmayer, Nature **563**, 225 (2018).
  - [17] M. Prüfer, *et al.*, Nature **563**, 217 (2018).
  - [18] D. C. Mattis, *The Theory of Magnetism Made Simple* (World Scientific, 2006).
  - [19] S. O. Demokritov, *et al.*, Nature **443**, 430 (2006).
  - [20] V. E. Demidov, *et al.*, Phys. Rev. Lett. **99**, 037205 (2007).
  - [21] A. V. Chumak, *et al.*, Phys. Rev. Lett. **102**, 187205 (2009).

- (2009).
- [22] M. Kollar, F. A. Wolf, and M. Eckstein, *Phys. Rev. B* **84**, 054304 (2011).
- [23] M. Marcuzzi, J. Marino, A. Gambassi, and A. Silva, *Phys. Rev. Lett.* **111**, 197203 (2013).
- [24] B. Bertini, F. H. L. Essler, S. Groha, and N. J. Robinson, *Phys. Rev. Lett.* **115**, 180601 (2015).
- [25] A. A. Serga, *et al.*, *Nature Communications* **5**, 3452 (2014).
- [26] A. J. E. Kreil, *et al.*, *Phys. Rev. Lett.* **121**, 077203 (2018).
- [27] L.-M. Duan, E. Demler, and M. D. Lukin, *Phys. Rev. Lett.* **91**, 090402 (2003).
- [28] S. Trotzky, *et al.*, *Science* **319**, 295 (2008).
- [29] B. Yan, *et al.*, *Nature* **501**, 521 (2013).
- [30] C. V. Parker, L.-C. Ha, and C. Chin, *Nature Physics* **9**, 769 (2013).
- [31] S. Hild, *et al.*, *Phys. Rev. Lett.* **113**, 147205 (2014).
- [32] C.-L. Hung, A. González-Tudela, J. I. Cirac, and H. J. Kimble, *Proc. Natl. Acad. Sci.* **113**, E4946 (2016).
- [33] E. J. Davis, G. Bentsen, L. Homeier, T. Li, and M. H. Schleier-Smith, *Phys. Rev. Lett.* **122**, 010405 (2019).
- [34] F. J. Dyson, *Phys. Rev.* **102**, 1217 (1956).
- [35] J. Xiao, G. E. W. Bauer, K.-c. Uchida, E. Saitoh, and S. Maekawa, *Phys. Rev. B* **81**, 214418 (2010).
- [36] M. Agrawal, V. I. Vasyuchka, A. A. Serga, A. D. Karenowska, G. A. Melkov, B. Hillebrands, *Phys. Rev. Lett.* **111**, 107204 (2013).
- [37] A. G. Gurevich and G. A. Melkov, *Magnetization oscillations and waves* (CRC Press, 1996).
- [38] C. L. Degen, F. Reinhard, and P. Cappellaro, *Rev. Mod. Phys.* **89**, 035002 (2017).
- [39] T. van der Sar, F. Casola, R. Walsworth, and A. Yacoby, *Nat Commun* **6**, 7886 (2015).
- [40] C. Du, T. van der Sar, T. X. Zhou, P. Upadhyaya, F. Casola, H. Zhang, M. C. Onbasli, C. A. Ross, R. L. Walsworth, Y. Tserkovnyak, and A. Yacoby, *Science* **357**, 195 (2017).
- [41] M. S. Grinolds, S. Hong, P. Maletinsky, L. Luan, M. D. Lukin, R. L. Walsworth, and A. Yacoby, *Nat Phys* **9**, 215 (2013).
- [42] B. Flebus and Y. Tserkovnyak, *Phys. Rev. Lett.* **121**, 187204 (2018).
- [43] J. F. Rodriguez-Nieva, D. Podolsky, and E. Demler, arXiv:1810.12333.
- [44] F. K. K. Kirschner, F. Flicker, A. Yacoby, N. Y. Yao, and S. J. Blundell, *Phys. Rev. B* **97**, 140402 (2018).
- [45] J. F. Rodriguez-Nieva, K. Agarwal, T. Giamarchi, B. I. Halperin, M. D. Lukin, and E. Demler, *Phys. Rev. B* **98**, 195433 (2018).
- [46] S. Chatterjee, J. F. Rodriguez-Nieva, and E. Demler, *Phys. Rev. B* **99**, 104425 (2019).
- [47] V. Zakharov, V. Lvov, and G. Falkovich, *Kolmogorov Spectra of Turbulence I: Wave Turbulence*, (Springer Berlin Heidelberg, 1992).
- [48] S. Nazarenko, *Wave Turbulence*, Lecture Notes in Physics (Springer Berlin Heidelberg, 2011).
- [49] D. D. Sheka, I. A. Yastremsky, B. A. Ivanov, G. M. Wysin, and F. G. Mertens, *Phys. Rev. B* **69**, 054429 (2004).
- [50] Y.-Q. Li, Y.-H. Liu, and Y. Zhou, *Phys. Rev. B* **84**, 205123 (2011).
- [51] M. Babadi, E. Demler, and M. Knap, *Phys. Rev. X* **5**, 041005 (2015).
- [52] S. M. Davidson and A. Polkovnikov, *Phys. Rev. Lett.* **114**, 045701 (2015).
- [53] J. Schachenmayer, A. Pikovski, and A. M. Rey, *Phys. Rev. X* **5**, 011022 (2015).
- [54] B. Zhu, A. M. Rey, and J. Schachenmayer, arXiv:1905.08782.